

Development and Performance Evaluation of Active Insulation Systems using Solid-State Thermal Switches

Emishaw Iffa, PhD
Member ASHRAE

Mikael Salonvaara
Member ASHRAE

Niraj Kunwar, PhD
Member ASHRAE

Som Shrestha, PhD
Member ASHRAE

Philip Boudreaux
Member ASHRAE

Diana Hun, PhD

ABSTRACT

Traditional building envelopes have passive insulation systems that cannot respond to dynamic changes in the environment. An Active Insulation System (AIS) consists of Active Insulation Materials (AIMs) that dynamically vary the thermal conductivity of the insulation system. Several researchers have evaluated the impact of AIS on building thermal and energy performance by using simulation tools. Up to 70% savings in annual heating and cooling energy and significant reductions in peak demand have been predicted for some climates with wall systems employing AIS. However, materials and assembly development have not yet achieved a cost-effective product that achieves the required performance. In this study, we present the process to develop an AIS that we will install in a test hut for its performance evaluation. Minimum performance criteria of the AIS system are developed based on R_{min}/R_{max} ratio, required time and efficiency to switch states, and cost estimates. The next steps carried out during this study are creating the concept to meet the requirements, predicting the performance via simulations, developing the experimental setup for bench-scale testing, and finally, constructing a full-scale wall assembly and monitoring the performance when exposed to natural weather conditions. The selected approach uses off-the-shelf products to create an AIS that can switch R -value between $\sim 1 \text{ ft}^2 \cdot \text{°F} \cdot \text{h} / \text{BTU}$ ($0.18 \text{ m}^2 \cdot \text{K} / \text{W}$) and $\sim 7 \text{ ft}^2 \cdot \text{°F} \cdot \text{h} / \text{BTU}$ ($1.23 \text{ m}^2 \cdot \text{K} / \text{W}$) and have a switching time of less than one minute between R -high and R -low.

INTRODUCTION

EIA's 2022 Energy Outlook shows commercial and residential buildings in the U.S. used more than 20 quadrillions BTU in 2021. This energy consumption is predicted to increase to 13 quads BTU and 10 quads BTU for residential and commercial buildings, respectively, by 2050 (EIA Annual Outlook, 2022). In addition, buildings generate about 40% of annual global CO₂ emissions, and 28% of these emissions are due to the operation of buildings. In 2016, HVAC loads contributed to 30% and 38% of the CO₂ emissions in commercial and residential buildings, respectively (Leung, J. 2018).

To decarbonize buildings and enhance energy savings, renewable energy sources such as solar and wind are considered

All authors are researchers at Building Envelope Materials Group, Buildings and Transportation Sciences Division, Oak Ridge National Laboratory, Oak Ridge, TN.

This manuscript has been authored by UT-Battelle, LLC, under Contract No. DE-AC05-00OR22725 with the U.S. Department of Energy. The United States Government retains and the publisher, by accepting the article for publication, acknowledges that the United States Government retains a non-exclusive, paid-up, irrevocable, world-wide license to publish or reproduce the published form of this manuscript, or allow others to do so, for United States Government purposes. DOE will provide public access to these results of federally sponsored research in accordance with the DOE Public Access Plan (<http://energy.gov/downloads/doe-public-access-plan>).

viable options. However, harvesting, storing, and consuming energy when needed requires ‘intelligent’ solutions. Active insulation systems can facilitate automated energy storage from renewable sources to a thermal storage unit and the release of the stored energy into the living space to complement or replace the conventional HVAC sources.

Simulation studies show that AIS integrated walls can contribute significantly toward energy savings. Park et al. (2015) found that residential buildings in climate Zone 5 have the potential to reduce cooling energy load by 30%. Antretter et al. (2019) showed that residential prototype buildings (Kneifel, 2012) for eight cities in different climate zones could achieve annual savings that ranged from 4096 KBtu to 8433KBtu (1192 to 2471 kWh). Residential buildings in the United States’ mild climate zones could save up to 45% in heating and cooling energy consumption (Menyhart et al., 2017). Several recent experimental (Atkins et al. 2022, Dabbagh et al., 2020, Gu et al., 2019, Pflug et al., 2017) and simulations (Iffa et al., 2022, Iffa et al., 2021, Carlier et al., 2020, Garriga et al., 2020, Antretter et al., 2019, Jin et al., 2017, Menyhart et al., 2017, Garriga et al., 2020) works show that not only can active insulation systems elevate energy savings, but it can have a significant impact in peak-load energy shaving. To achieve high-performance active insulation systems, some potential advanced solutions to develop effective dynamically varying insulation solutions are recommended (Iffa et al., 2022, Gu et al., 2019, Kisilewicz et al., 2020).

Eventhough, the above studies show the AIS potential of energy savings and peak demand reduction, there are no case-specific AIS selection protocols and the minimum expected performance metrics. This paper discusses an AIS performance specification, selection criteria, and the respective development of an AIS prototype. The performance of the AIS prototype was tested in a heat flow meter (HFM), and the results were used to validate simulation models that were used to extrapolate findings to optimize AIS parameters for performance enhancement. Finally, a currently monitored, 4 ft × 8 ft (1.2 m × 2.4 m) AIS wall design and construction procedures are discussed.

AIS PARAMETERS SELECTION CRITERIA

Key parameters such as minimum R-value (R-low) and maximum R-value (R-high), response time, amount of energy needed to change the R-value state, ease of assembly and integration into buildings, robustness, longevity, and the construction and running costs were used as selection criteria to evaluate the proposed AIS concepts.

To assign percentage weight to each AIS performance evaluation criteria, a minimum requirement for functionality, performance, and cost expected of the AIS system is set and shown in Table 1. The R-high and R-low values are selected based on achieving 70% of typical rigid insulation during R-high and having conductive insulation of $\sim R-1$ during the R-low state. Our computational study shows any switching time lower than half an hour provides similar performance. Thus, a 5-minute switching time is set as a minimum switching criteria. A small motor power requirement is used to select the efficiency of switching. The minimum cost estimate is selected based on a combined cost of AIS components, actuating mechanisms and cost of power demand.

Table 1. Minimum Required Property of the AIS Material

Property	Desired
Rmin/Rmax@thickness	Rmin ~ 1 / Rmax > 7 @ < 2 in (Rmin ~ 0.176 K·m ² /W / Rmax > 1.233 K·m ² /W @ 50.8mm)
Time to switch states	< 5 min
Actuator	Durable, simple
Efficiency of switching	< 1 Wh / ft ² (< 10.8 Wh/m ²)
Cost estimate / ft ²	$< \$5$ /ft ² ($< \$53.8$ /m ²)

ACTIVE INSULATION SYSTEM USING SOLID-STATE THERMAL SWITCH

The Solid-state thermal switch (STS) that uses different ways of connecting and disconnecting metallic (or other highly conductive) strips have a potential of providing varying low and high R-values to a system. The range of Rmin/Rmax can be significantly varied and depends on the spacing of the thermal bridges. The AIS system with STS was selected for a test based on the performance (R-min to R-high ratio), construction cost, ease of buildability, and scalability.

The AIS system’s working principle uses a metal connector design to switch the active insulation between R-high and R-low. Low-emittance connectors disengage from the interior and exterior cover foils to avoid thermal bridging when the

insulation is in an R-high state.

In the R-low state (conducting), the system opens the connectors in the cavity allowing conduction along the connectors. The connectors will be made of aluminum or similar material that has high thermal conductivity. Additionally, the system has highly conductive aluminum foils on both the exterior and interior sides of the insulation to allow the heat to spread on the surface and enhance the heat transfer rate.

The Final AIS wall system will comprise two interior and exterior active insulation assemblies on both sides of a fully grouted concrete masonry unit (CMU). The CMU core will be used for thermal energy storage.

AIS Prototype Design

As a proof of concept, a 24 in × 24 in (60 cm × 60 cm) AIS prototype was built, which consisted of 2-in-thick (50.8 mm) extruded polystyrene (XPS) insulation and three 2-inch-wide U-channel aluminum foils (shown in red in Figure 1). Aluminum foils with 24 in × 24 in and 10 mil in thickness (60 cm × 60 cm and 0.254 mm thickness) were placed on both sides of the XPS as shown in Figure 1. Table 2 shows the material properties of the XPS and the aluminum foil used in this study. The AIS system is at R-low when the U-channel aluminum foils engage with the top and bottom aluminum foils and create a thermal bridge between them that increases the effective thermal conductivity of the AIS. Conversely, the R-high state is attained when the U-channels are disengaged from the aluminum foils. An air gap of 3 in (76.2 mm) is left in the middle of AIS to allow the U-channels to engage (R-low) and disengage (R-high) on demand.

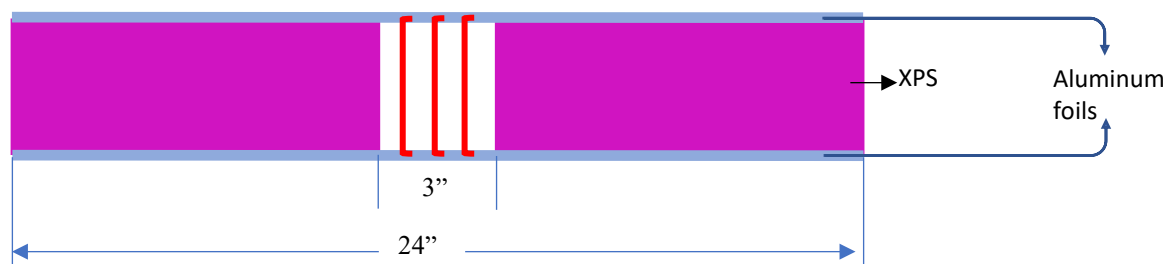


Figure 1. Schematic drawing of the AIS system prototype.

Table 2. Material Properties of the Main AIS Components

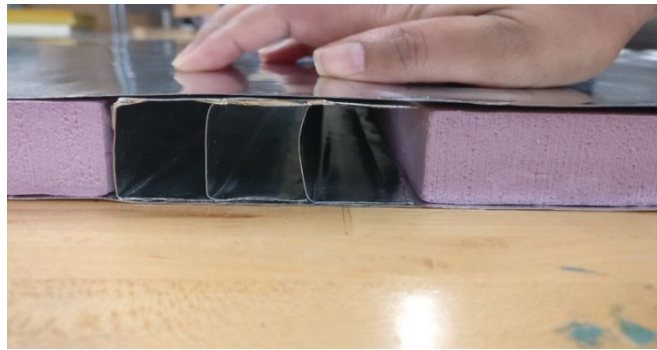
Material	Thermal conductivity (W/m.K) / (Btu- in/hr.ft ² .°F)	Heat capacity (J/kg.K) / (Btu/(lb.°F))	Density (kg/m ³) / (lb/ft ³)
Aluminum foil	220 /1526	900 /0.215	2700 /168.55
XPS	0.029/ 0.201	1470 /0.351	28.6 /1.785

Laboratory HFM test

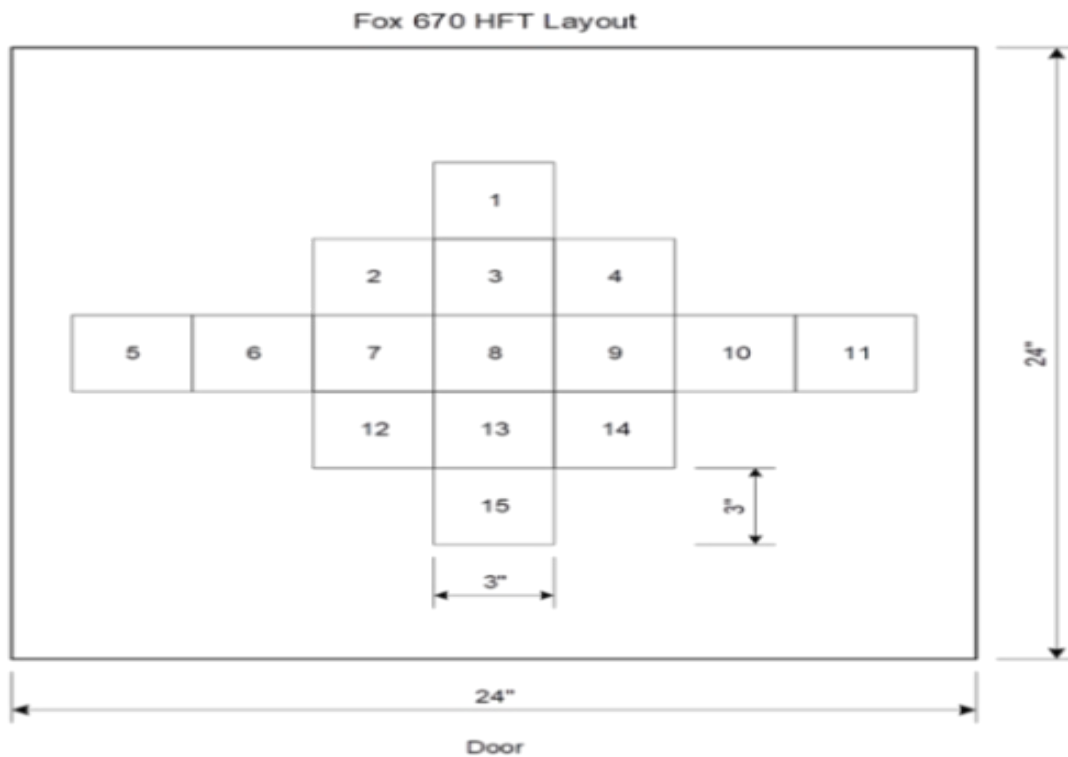
The AIS design for the R-low state was tested in the FOX 670 heat flow meter apparatus in steps to investigate the impact of the individual AIS components on the system. Two pieces of 10.5" × 24" (26.67cm) XPS insulation were spaced 3" apart in the middle to leave an air gap to give space for the AIS metal strips a space for movement, as shown in Figure 2 (a).

Initially, the system was tested with 10 mil-thick (0.254 mm) aluminum foils covering both sides of the insulation. The three U-channel strips were removed from the air gap to create the R-high state. Finally, the U-channels were placed in the air gap and in contact with the foils on both sides of the XPS, creating a thermal bridge and R-low state.

The FOX 670 heat flow meter (HFM) that was used has the capability of taking localized heat flux measurements. The HFM has 15 sensors, each having a measuring area of 3" × 3" (76.2 mm × 76.2 mm) and are arranged as in Figure 2 (b). Sensors 5, 6, 7, 8, 9, 10, and 11 measure the heat flux and thermal conductivity of the AIS system from left to right either on the XPS and aluminum foil composite or the AIS strip in the middle. Whereas sensors 1, 3, 8, 13, and 15 measure the heat flux and thermal conductivity of the AIS strip in the middle.



a)



b)

Figure 2. a) AIS test specimen prepared at R-low. b) Sensor layout of FOX 670 heat flow meter.

Simulation Design

Simulations were run to reproduce the Heat Flow Meter (HFM) measurement for validation purposes and further optimize the AIS specifications used in the wall design and construction. An AIS system with 1" thick XPS and 10 mil aluminum foils was simulated and validated with the HFM test. The COMSOL Multiphysics 6.0 Heat Transfer and Surface-to-Surface Radiation modules were used to compute the effective heat flux and the nominal R-values at the R-low and R-high states. The boundary conditions on the sides of the test samples were set to 12.8°C and 35°C just as these were set in the HFM. Based on parametric simulations, the thickness of the aluminum foils and the number of the aluminum U-channels that more effectively enabled R-low and R-high were set.

RESULTS AND DISCUSSION

This section compares the simulation and experimental results for validation purposes. In addition, HFM experimental measurements and extrapolated simulation results are presented and discussed to show the capability of the R-low and the R-high ratios under different parameters. Finally, the newly constructed wall manufacturing plan is discussed.

Validation of simulation results

The heat flux measurements of the test sample were recorded and compared with the simulation values. Heat flux measured values by sensors 5-11 (labeled in Fig. 2(b)) were compared with the average heat flux simulation results every 3" (76.2 mm) across the mid-section from left to right for the R-low case with the 1" thick XPS foam covered with 10 mil aluminum foil at the top and the bottom. Sensor 5 covers the distance from 1.5"- 4.5" (38.1 mm - 114.3 mm) from the left, while sensor 6 spans 4.5"-7.5" (114.3 mm – 190.5 mm) from the left, and so on. Sensor 8 represents the heat flux measurement at the center and around the symmetry line of the setup.

Figure 3 shows that simulation results have good agreement with the experimental data. The average percent error between the measured and simulated results was 4.4%.

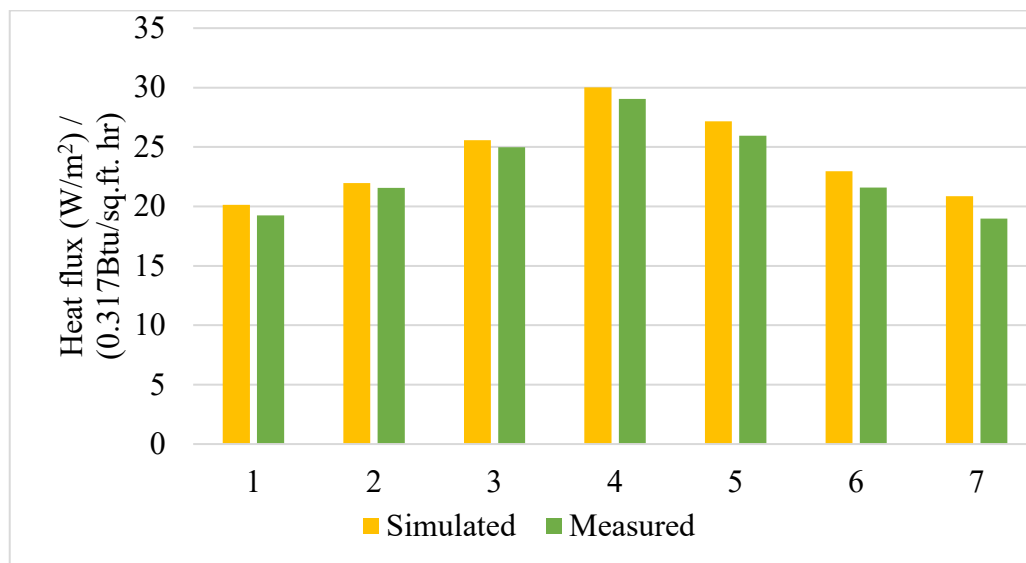


Figure 3. Heat flux measurement and simulation values from the AIS prototype at heat flux locations at 3" increments, sensors labeled in 2 (b).

Laboratory test and extrapolated simulation results

The AIS test specimen was built with materials and specifications discussed in the wall design section. To improve the accuracy of the HFM measurement, silicone mats with known thermal conductivity were placed at the top and bottom of the AIS. Additionally, 3/4" (19 mm) thick XPS foam on the top of the AIS is placed, and the heat flux values and their respective thermal conductivity of the AIS system were measured in three steps. As the first step in measuring the R-high state, the three aluminum strips in the middle (in the air gap) were not connected to the top and bottom layers of the aluminum foils. To differentiate the effects of radiation from heat conduction due to thermal bridging of the aluminum strips, this step was repeated with aluminum foils having an inner side of dark paint and a shiny surface at the middle air gap. The last test conducted was the R-low case with the three aluminum strips in contact with the aluminum foils.

The heat flux measurements of the AIS system together with the silicone mats and 3/4" XPS were measured together. While computing the R-values of the AIS system, the R-values of the mats and the additional XPS board are subtracted, as shown in Equation 1. Table 3 shows the heat flux measurements from each sensor in the HFM, the average heat flux of the AIS mid-section, and the computed R-values of the AIS system under different R-states (R-high and R-low). The hot and cold plate

temperatures of the HFM were 35°C and 12.8°C with temperature differential (ΔT) of 22.2°C.

$$R_{AIS} = \frac{l \cdot \Delta T}{q_{tot}} - 2R_{mat} - R_{XPS} \tag{1}$$

Table 3. Heat Flux Measurements by Each Sensor in the HFM, Average Heat Flux in Mid-section, and R-values of the AIS

R-state	Heat flux measurements in each sensor (Figure 2(b)) (W/m ²) / (Btu/sq.ft. hr)							Average heat flux across mid section (W/m ²) / (Btu/sq.ft. hr)	R _{AIS} (°F·ft ² ·h/Btu) / (K·m ² /W)
R-low				50.75					
				16.1					
			24.58	48.06	29.35				
			7.79	15.2	9.3				
	17.89	18.42	24.69	48.49	29.60	18.36	18.03		
		5.67	5.84	7.89	15.4	9.38	5.82	5.72	
			23.87	50.49	29.67				
			7.57	16	9.41				
			48.90						
			15.5						
							25.07		1.34
							7.92		0.236
R-high and inner Al foil surface dark painted				24.48					
				7.76					
			19.97	24.88	19.52				
			6.63	7.89	6.12				
	17.51	16.91	20.66	24.10	19.94	16.32	17.26		
		5.55	5.36	6.55	7.64	6.32	5.37	5.47	
			20.64	25.77	20.29				
			6.54	8.17	6.43				
			23.70						
			7.51						
							18.95		2.99
							6.01		0.527
R-high				13.06					
				4.14					
			13.23	13.03	13.16				
			4.19	4.13	4.17				
	12.83	12.89	13.25	13.10	13.08	12.63	12.88		
		4.07	4.09	4.21	4.15	4.15	4.0	4.08	
			13.13	13.28	13.24				
			4.16	4.21	4.2				
			13.16						
			4.17						
							12.95		4.19
							4.11		0.738

As shown in Table 3, the average heat flux (and their respective R values) for R-low, R-high with dark paint, and R-low with shiny surfaces were found to be 25.14 W/m² (R-1.34), 18.95 W/m² (R-2.99) and 12.95 W/m² (R-4.19), respectively.

A COMSOL Multiphysics simulation was run for identical material properties, geometry, and boundary conditions to compute the R-values of the AIS under R-low and R-high conditions. The simulation results were compared with the experimental results, and additional parameters were varied to optimize the R-high to R-low ratio. Two parameters, namely, the thicknesses of the rigid insulation and the aluminum foils, were varied. The XPS thickness was varied between 1” (25.4

mm), 1.5" (38.1 mm), and 2" (50.8mm), and the thickness of the aluminum foils used was 10 mil and 20 mil foils. As shown in Table 4, the simulated and measured data agree well. The rigid foam provides R-4.3/in without the AIS. We used 20 mils (0.51 mm) aluminum foils with 2" (50.8 mm) rigid foam insulation that attained R-8.2 in the R-high and R-1.1 in the R-low states, which led to a Rmax/Rmin ratio of 7.5.

Table 4. Measured and Simulated R-values of the AIS System under R-low and R-high States.

Set up	R-values ($^{\circ}\text{F}\cdot\text{ft}^2\cdot\text{h}/\text{Btu}$) / ($\text{K}\cdot\text{m}^2/\text{W}$)				
	Measured 1"	Simulated 1"	Simulated 1.5"	Simulated 2", 10 mil	Simulated 2", 20 mil
R-high	4.2 / 0.740	4.3 / 0.757	6.3 / 1.109	8.2 / 1.444	8.2 / 1.444
R-low	1.4 / 0.247	1.3 / 0.229	1.5 / 0.2641	1.5 / 0.2641	1.1 / 0.2641
R-high/R-low	3.0 / 0.528	3.3 / 0.581	4.2 / 0.740	5.5 / 0.969	7.5 / 1.321

AIS wall design for large-scale environmental chamber test

The previous sections were dedicated to showing that the Rmax/Rmin ratio could be achieved based on HFM and simulation tests. This section focuses on the design of scaled-up and automated wall to test a fast R-states' varying capability and the AIS durability. For ease of swinging between R-high and R-low, the fixed U-channels in the HFM test are replaced by movable flat pieces and pairs of fixed U-channels as shown in Figure 4. A 4 ft × 8 ft (1.2 m × 2.4 m) AIS system was designed to be tested under a Guarded Hot Box. the active insulation is constructed of pairs of aluminum sheets, aluminum U-channels and moving aluminum pieces to engage and disengage with the U-channels. The active insulation is placed in six equidistant positions and the remaining gap is filled with XPS foam. Figure 4 (a) shows the R-low state where the flat pieces are engaged with the U-channels to create a thermal bridge and a higher heat flow through the AIS. In The R-high state, with the lack of contact between the metal pieces creates a thermal break to allow a smaller amount of heat flow through the AIS system, Figure 4 (b).

The movement of the flat piece is limited using a couple of stoppers during R-high states. Springs are placed between the stopper and flat piece to provide some tolerance in case all the flat pieces are not at the same distance from the U-channel leg.

The control system uses a linear motion of flat aluminum pieces to engage/disengage with the U-channels. The flat pieces are suspended in a steel wire which is clamped to a shaft. The shaft is rotated using a DC motor and the wire clamped to the shaft converts the rotary motion into linear motion. The DC motor is controlled using the signal sent by the data acquisition system/controller based on the control logic and the sensor input from the thermistors connected at the surface of the AIS The construction of the test wall will be completed in September 2022. Afterwards, it will be monitored in the Guarded hot Box for an extended period under different climate conditions and R-state schedules.

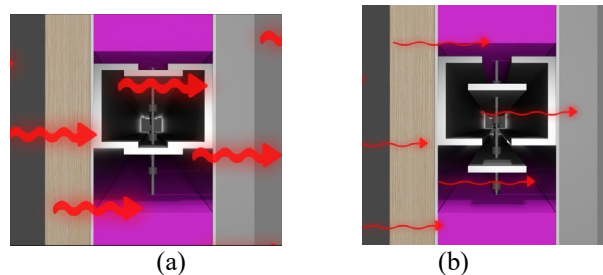


Figure 4 (a) The R-low state, flat pieces engaged with U-channels (b) R-high state, when there is no contact between the flat pieces and U-channels.

CONCLUSION

In this study, AIS selection criteria and AIS concept evaluation procedures were discussed. A solid-state thermal switch consisting of mechanically moving metal strips combined with a rigid insulation concept was selected. A proof of concept of the design was constructed and tested in heat flow meter apparatus with multiple sensors. The results obtained are used to calibrate a COMSOL model of the AIS system; the average percent error was 4.4%. A 2 in (50.8 mm) thick XPS integrated with 20 mil aluminum foils provides an R-high of 8.2 $\text{ft}^2\cdot^{\circ}\text{F}\cdot\text{h}/\text{BTU}$ (1.44 $\text{W}^2\cdot\text{m}/\text{K}$) and an R-low of 1.1 $\text{ft}^2\cdot^{\circ}\text{F}\cdot\text{h}/\text{BTU}$ (0.19 $\text{W}^2\cdot\text{m}/\text{K}$) $\text{ft}^2\cdot^{\circ}\text{F}\cdot\text{h}/\text{BTU}$. Based on this study, a 4 ft × 8 ft (1.2 m × 2.4 m) AIS wall is being constructed and instrumented to

monitor its performance.

ACKNOWLEDGMENTS

This manuscript has been authored in part by UT-Battelle, LLC, under contract DE-AC05-00OR22725 with the US Department of Energy (DOE). The publisher acknowledges the US government license to provide public access under the DOE Public Access Plan (<http://energy.gov/downloads/doe-public-access-plan>).

The authors are grateful for the support from Jerald Atchley during the construction of the prototype.

NOMENCLATURE

ΔT	=	upper and lower HFM temperature difference
l	=	overall thickness of the AIS
R_{AIS}	=	R-value of the AIS
R_{mat}	=	R-value of the silicone mats
R_{XPS}	=	R-value of the added XPS insulation
q_{tot}	=	total heat flux

REFERENCES

- Antretter, F. Hun, D.E., Boudreaux, P.R., Cui, B. Assessing the Potential of Active Insulation Systems to Reduce Energy Consumption and Enhance Electrical Grid Services, Oak Ridge National Laboratory, Oak Ridge, Tennessee United States, 2019.
- Atkins, C., Hun, D., Im, P., Post, B., Slattery, B., Iffa, E., ... & Lapsa, M. V. (2022). Empower Wall: Active insulation system leveraging additive manufacturing and model predictive control. *Energy Conversion and Management*, 266, 115823.
- Dabbagh, M., Krarti, M. Evaluation of the performance for a dynamic insulation system suitable for switchable building envelope, *Energy Build.* 222 (2020), 110025.
- Carlier, R., Dabbagh, M., Krarti, M. Impact of wall constructions on energy performance of switchable insulation systems, *Energies* 13 (2020) 6068.
- Garriga, S.M., Dabbagh, M., Krarti, M. Evaluation of dynamic insulation systems for residential buildings in Barcelona, Spain, *ASME J. Eng. Sustain. Build. Cities* 1 (1) (2020), 011002.
- Gu, B., Liang, K., Zhang, T., Yue, X., Qiu, F., Yang, D., Chen, M. Fabrication of sandwich-structured cellulose composite membranes for switchable infrared radiation, *Cellulose* 26 (2019) 8745–8757.
- Iffa, E., Hun, D., Salonvaara, M., Shrestha, S., & Lapsa, M. (2022). Performance evaluation of a dynamic wall integrated with active insulation and thermal energy storage systems. *Journal of Energy Storage*, 46, 103815.
- Iffa, E., Salonvaara, M., & Hun, D. (2021, November). Energy performance analysis of smart wall system with switchable insulation and thermal storage capacity. In *Journal of Physics: Conference Series* (Vol. 2069, No. 1, p. 012092). IOP Publishing.
- Jin, Q., Favoino, F., Overend, M. Design and control optimisation of adaptive insulation systems for office buildings. Part 2: a parametric study for a temperate climate, *Energy* 127 (2017) 634–649.
- Kneifel, J. (2012). *Prototype Residential Building Designs for Energy and Sustainability Assessment*. US Department of Commerce, National Institute of Standards and Technology.
- Leung, J. (2018). *Decarbonizing US buildings*. Center for Climate and Energy Solutions.
- Kisilewicz T., Fedoreczak-Cisak M., and Barkanyi T. 2019 Active thermal insulation as an element limiting heat loss through external walls *Energy Build* 205 109541.
- Menyhart, M., Krarti, K., Potential energy savings from deployment of dynamic insulation Materials for US residential buildings, *Build. Environ.* 114 (2017) 203–218.
- Park, B., Srubar, W.V., Krarti, M. Energy performance analysis of variable thermal resistance envelopes in residential buildings, *Energy Build.* 103 (2015) 317–325.
- Pflug, T., Bueno, B., Siroux, M., Kuhn, T.E. Potential analysis of a new removable insulation system, *Energy Build.* 154 (2017) 391–403.
- U.S. Energy Information Administration, *Annual Energy Outlook 2022* (Washington DC: U.S. department of energy, 2022), <https://www.eia.gov/outlooks/aeo/>